Electrical performance of a low inductive 3.3kV half bridge IGBT module

*Modern converter concepts demand increasing energy efficiency and flexibility in design and construction. Beside low losses, a minimized commutation inductance for clean switching is desirable. A general concept for a low inductive and highly symmetric half bridge IGBT module for high power applications has been worked out and introduced as the new high power module platform called XHP (Fle**X**ible **H**igh-Power **P**latform).*

By Sven Buchholz, Matthias Wissen, Thomas Schütze, Infineon Technologies AG

The XHP Scope

XHP is a new housing platform for high power IGBT modules developed mainly for industrial drives, traction, renewable energy and power transmission. Its scalability simplifies converter design and manufacturing. Due to its robust architecture, the XHP provides long-term reliability in applications with demanding environmental conditions.

Driving forces in the implementation of the XHP are the demand for flexibility, increasing power density, efficiency, reliability and robustness, which are addressed by the following approach:

- The modular concept enables scalability with high current density at a low system stray inductance
- The half bridge switch configuration reduces system cost while it provides increased power density and reduced losses
- The electrical and mechanical module design yields switching symmetry, a low internal stray inductance and enables an overall low inductance in the DC bus
- State-of-the-art joining techniques like ultrasonic welding connections ensure highest reliability and durability
- The future-oriented platform design prepares for the next joining and chip technologies, which will further enhance power density, life time and load cycle capability

The XHP HV Design

The high voltage XHP HV module with up to 10.4 kV insulation and corresponding creepage distances is designed as a package for voltage classes of 3.3 kV and above. It is dimensioned to fit the footprint of today´s IHV-A and IHV-B modules: due to the unchanged depth of 140 mm identical extruded heat sink profiles can be used. Four modules with a foot print of 140x100 mm², mounted without a gap by alignment hooks, will exactly fit into today's space of two 140x190 mm² IHV modules.

In contrast to existing platforms, the XHP is characterized by its modular concept that leads to a considerable flexibility. The single module becomes a building block for systems with higher current ratings with an excellent internal and external current sharing. Paralleling of four XHP HV devices is sketched in Figure 1 and compared to two IHV-B modules in half bridge configuration. The DC-link terminals offer a simply structured connection to the capacitor bank, and the AC terminals can be paralleled by a single bar. The area in between is designated for an interconnecting PCB carrying drivers or booster stages.

Due to an internal relative commutation inductance (the product of inductance L_s and nominal current I_{nom}) between upper and lower switch of only $L_s \cdot I_{nom}$ = 11 µHA for a 450 A rated 3.3 kV XHP HV module and a low inductive bus bar design an impressively low overall stray

inductance can be realized: For four parallel 3.3 kV XHP modules with a total current rating of 1800 A, a total commutation inductance of less than 15 nH can be achieved. For comparison, the typical, yet low L_s of an IHV-B based half bridge of 1500 A current and 3.3 kV voltage rating amounts to roughly 90 nH.

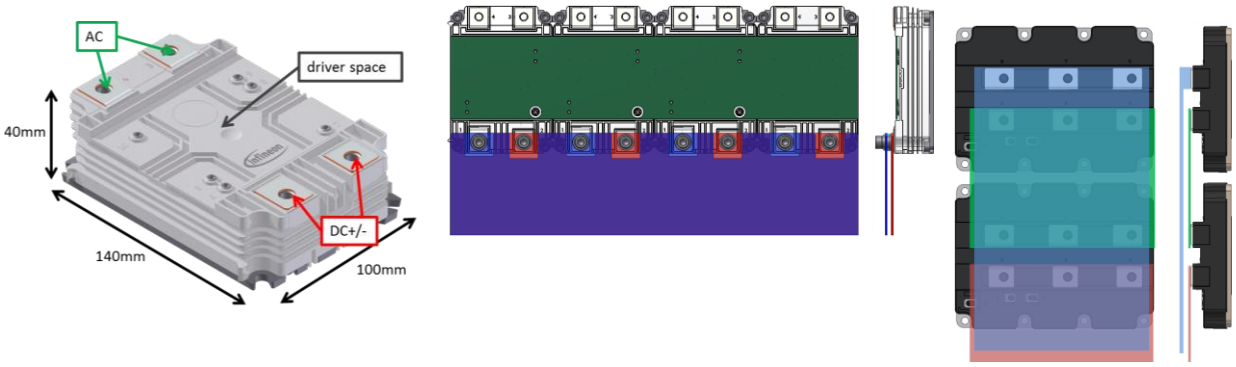

Figure 1: High voltage IGBT package XHP HV. Schematic top and side views with sketched DC+/- bus of four paralleled XHP HV modules and two IHV-B modules in half bridge configuration

The XHP HV Electrical Performance

The implementation of a low inductive and highly symmetric half bridge design offers several benefits regarding the module´s switching behavior on the one hand and the converter's performance on the other hand. Major advantages over typical contemporary module and converter designs are:

- reduced commutation inductance due to the internally optimized commutation path within the half bridge module
- reduced dynamic losses with potential for higher converter switching frequencies
- reduced voltage overshoot at IGBT and diode and soft, oscillation-free switching even at fast turn-on and turn-off
- reduced risk of IGBT and diode current snap-off and oscillation behavior

In the following sections an insight into the switching characteristics and the dynamic losses of the 450 A rated 3.3 kV XHP HV in comparison to the 1500 A rated 3.3 kV IHV-B module, Infineon's FZ1500R33HE3 will be provided.

Both devices are equipped with 3rd generation Trench/Fieldstop IGBTs and Emitter Controlled diodes. Normalized to nominal current, the static IGBT and diode losses of the XHP and the IHV-B are equal.

The total commutation inductance of the XHP HV setup amounts to L_s = 85 nH or a relative stray inductance of $L_s \cdot I_{nom}$ = 38 µHA. As 25 nH of this inductance are attributed to the module itself, two times 30 nH arise from the capacitor bank and the bus bars. A typical IHV-B setup with nominal current I_{nom} = 1500 A has a total commutation inductance of L_s = 90 nH (or $L_s \cdot I_{nom}$ = 135 µHA). Hence, the XHP based setup features a relative stray inductance which is less than 30% of that of the IHV-B based setup.

Diode recovery and choice of IGBT turn-on resistance

The lower relative stray inductance of the XHP HV converter design allows faster diode recovery and IGBT turn-on switching compared to the IHV-B setup. The limitation for the IGBT turn-on speed arises from the diode's allowed maximum power dissipation during commutation. For a fixed switching speed $di/dt = -di_F/dt$ a lower stray inductance leads to a lower induced voltage peak $V_{F\,max} = L_s \cdot di_F/dt_{max}$ at diode recovery which in turn yields lower power dissipation.

Figure 2 a) compares the diode power dissipation during recovery for the XHP and IHV-B based converters as a function of the switching speed for a junction temperature of T_j = 125°C. Peak power P and di/dt are normalized by the respective maximum allowed diode power dissipation P_{RQM} and nominal current I_{nom}. For the IHV-B setup P/P_{RQM} rises steeply with the relative switching speed, and P_{RQM} is reached at $di/dt/I_{nom}$ = 4.0 μs^{-1}, i.e. di/dt = 6 kA/µs. Faster switching is not allowed as it endangers the diode.

In case of the XHP setup, P/P_{RQM} increases less steeply with the relative switching speed, and P_{RQM} is reached at $di/dt/I_{nom}$ = 12.3 μs^{-1} (di/dt = 5.5 kA/µs) which amounts to more than three times the IHV-B value. At nominal conditions (here $P = 0.6 \cdot P_{RQM}$) a factor of three applies as well. This behavior is directly related to the XHP's lower relative stray inductance. At T_j = 125°C, the nominal turn-on conditions for the XHP are thus defined for di/dt = 4.3 kA/µs ($di/dt/I_{nom}$ = 9.6 μs^{-1}), where the diode stress is equal to that of the nominally switched IHV-B.

Figs. 2 c-e) depict the diode current $-I_F$ and voltage V_F characteristics for different setups and conditions as indicated in Figure 2 a). The comparison of Figure 2 c) and d) illustrate the positive effect of the lower relative commutation inductance for the XHP setup.

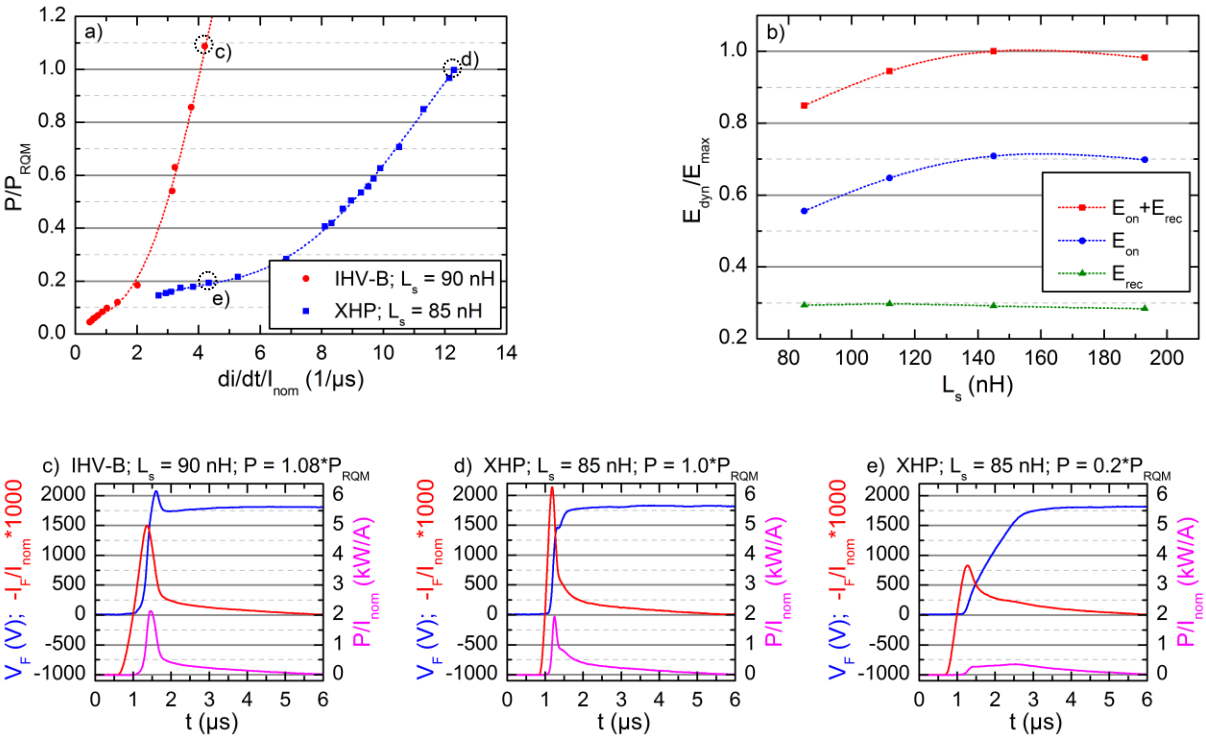

Figure 2: Diode recovery power dissipation for an XHP based and an IHV-B based converter with Ls·Inom = 38 and 135 µHA, respectively

a) Dissipated power P normalized by the respective allowed maximum PRQM, vs. di/dt, normalized by the respective nominal current

b) Normalized dynamic XHP IGBT and diode losses Eon and Erec at IGBT turn-on as a function of the total commutation inductance Ls at same diode power dissipation P (Tj = 25°C)

c,d) Measurements of the current -IF and voltage VF characteristics of IHV-B and XHP diode recovery at the respective SOA limit P = PRQM

e) XHP diode recovery with the same relative switching speed as for the IHV-B in c)

For the same diode stress P = P_{RQM} and two times faster switching, the XHP diode does not see any overvoltage peak. On the other hand the V_F characteristic of the IHV-B diode shows a pronounced overvoltage peak under this extreme condition. The measurement in Figure 2 e) and 2 c) allows the comparison of XHP and IHV-B diode recovery characteristics with the same relative switching speed $di/dt/I_{nom}$. The XHP diode stress is significantly reduced. However the IGBT turn-on losses E_{on} are 2.4 times as high as for the fast XHP switching with $di/dt/I_{nom}$ = 12.3 μs^{-1} in Figure 2 d).

In order to minimize the total dynamic losses at IGBT turn-on $E_{on}+E_{rec}$ and to guarantee a safe operating area (SOA) for the diode as usually defined for high power modules, diode power dissipation P_{diode} is chosen to be constant when changing the commutation inductance L_s. For the XHP, Figure 2 b) depicts the normalized dynamic losses as a function L_s for constant P_{diode} under nominal I_F, V_F and R_{Gon} conditions at T_j = 25°C. For each value of L_s the gate driver turn-on resistance R_{Gon} was tuned to meet equal $P_{diode} = 0.6 \cdot P_{RQM}$ values. While decreasing L_s does not change the dynamic diode losses E_{rec}, the IGBT losses E_{on} are significantly reduced. A decrease of L_s from 195 nH to 85 nH reduces $E_{on}+E_{rec}$ by 15%. While this approach yields the maximum of dynamic loss reduction, the individual application may require a trade-off between the reduction of E_{on} and E_{rec}. An even further reduction of dynamic losses is possible by the application of faster diodes with less recovery charge.

A low relative stray inductance $L_s \cdot I_{nom}$ contributes to an improved electromagnetic compatibility. This becomes evident under several typical switching conditions, e.g. whenever a steep di/dt may evoke V_F voltage spikes or oscillations. Figure 3 illustrates the diode recovery of the XHP under nominal R_{Gon}, increased V_F = 2300 V, low current $-I_F = 1/10 \cdot I_{nom}$ and T_j = 25°C in comparison with the respective IHV-B measurement. With the faster XHP switching the diode tail current declines smoother than the IHV-B's. This softness in combination with the lower $L_s \cdot I_{nom}$ prevents oscillations as observed in the corresponding IHV-B characteristic, and it allows the application of faster diodes with less recovery charge. The good oscillation behavior of the XHP application enhances electromagnetic compatibility and potentially reduces protective EMI measures in converter design.

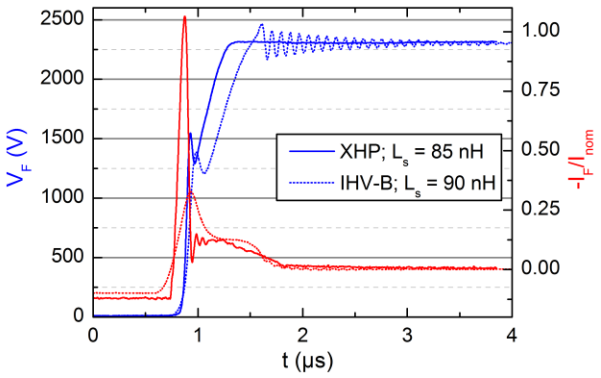

Figure 3: Comparison of XHP and IHV-B diode recovery characteristics at increased V_F = 2300 V, low current $-I_F = 1/10 \cdot I_{nom}$ and the respective nominal R_{Gon} at T_j = 25°C

IGBT turn-on

The IGBT turn-on speed is limited by the maximum allowed diode power dissipation during recovery. The XHP's nominal turn-on resistance is chosen accordingly. A comparison of the XHP and IHV-B turn-on characteristics under nominal conditions at T_j = 125°C is shown in Figure 4 a). The relatively faster switching of the XHP brings the benefit of an E_{on} reduction of 21% compared to the IHV-B turn-on.

The XHP's fast turn-on characteristic at nominal V_{CE} and I_C is plotted in Figure 4 b). This characteristic corresponds to the diode recovery measurement shown in Figure 2 d) with the diode at the P_{RQM} limit. The IGBT turn-on measurement shows a smooth gate voltage

characteristic V_{GE} without any signs of turn-on oscillations. Such oscillations cause electromagnetic noise in the application and are provoked by an asymmetrical module design and high speed switching.

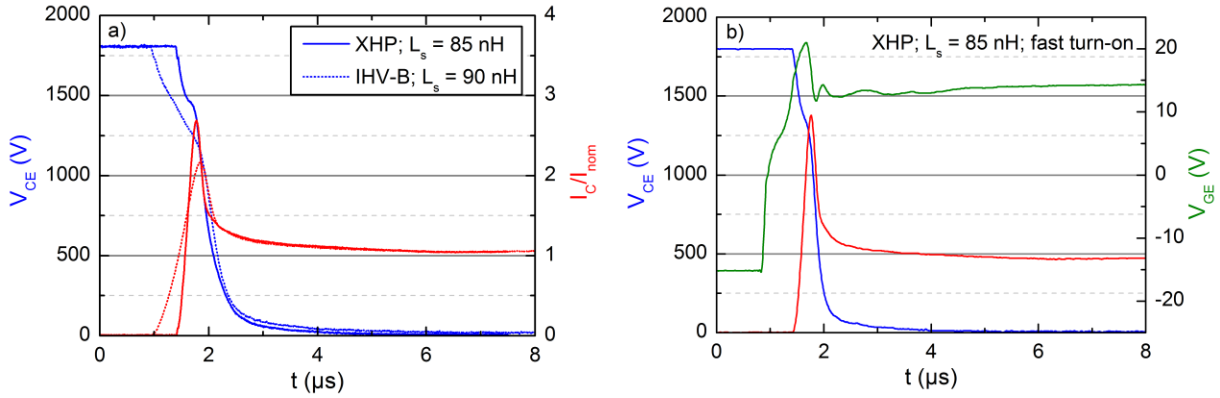

Figure 4: Comparison of XHP and IHV-B IGBT turn-on characteristics

a) nominal conditions at T_j = 125°C, XHP's E_{on} is reduced by 21% compared to the IHV-B

b) XHP's fast turn-on characteristic for nominal voltage and current at the diode P_{RQM} limit

IGBT turn-off

Since the IGBT turn-off speed is usually limited by the maximum allowed dv/dt_{max} of the application, we compare the turn-off characteristics of the XHP and the IHV-B setup under the same nominal dv/dt. Generally, an increase of dv/dt (i.e. smaller R_{Goff}) yields a faster turn-off di/dt, which in turn reduces the turn-off losses but evokes a higher over voltage peak $V_{CE\ max} = -L_s \cdot di/dt_{max}$.

A comparison of XHP and IHV-B IGBT turn-off measurements under nominal conditions at T_j = 125°C is presented in Figure 5 a). The same dv/dt at turn-off switches off the current I_C with the same normalized waveform. The resulting same $di/dt/I_{nom}$ generates a significantly lower over voltage peak in case of the lower inductive XHP setup. The over voltage peak height $V_{CE\ max} - V_{CE\ nom}$ is 32% smaller while the XHP's E_{off} turns out to be 5% lower than that one of the IHV-B.

Figure 5 b) compares switching under harsh conditions with increased V_{CE} = 2400 V, high current $I_C = 2 \cdot I_{nom}$ and nominal R_{Goff} at T_j = 25°C. For the IHV-B the maximum allowed voltage of 3300 V is slightly exceeded, i.e. the reverse bias RBSOA limit is reached. Since there is no tail current left at turn-off a light snap off behavior with V_{CE} oscillations is observed. On the other hand, the lower relative inductance of the XHP setup leads to a significantly lower voltage peak and a finite current tail. Snap off and electromagntic noise is suppressed and the voltage overshoot does not violate the RBSOA limit.

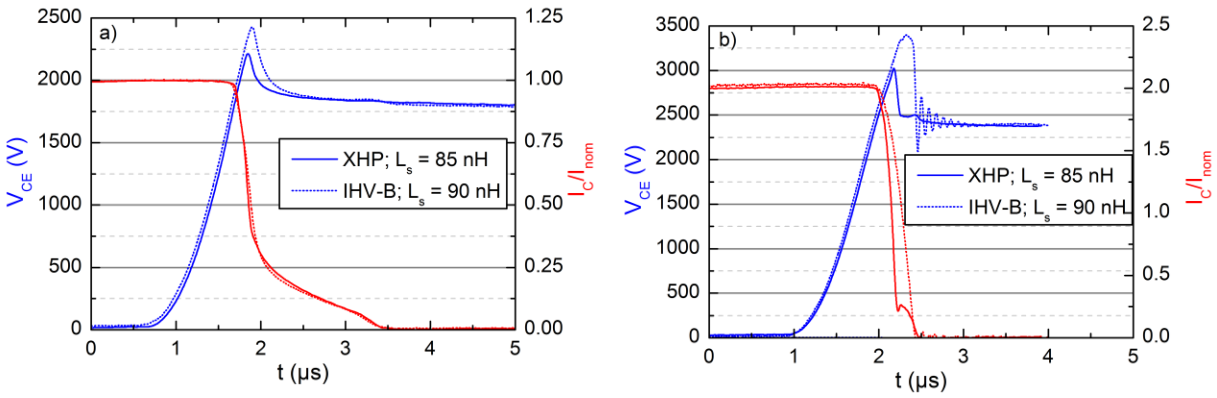

Figure 5: Comparison of XHP and IHV-B IGBT turn-off characteristics

a) nominal conditions at T_j = 125°C

b) increased V_{CE} = 2400 V, high current $I_C = 2 \cdot I_{nom}$ and nominal R_{Goff} at T_j = 25°C

Figure 6 a) illustrates the influence of the lower relative stray inductance on the over voltage peak $V_{CE\,max}$ for different dv/dt values. $V_{CE\,max}$ rises less steeply with increasing dv/dt in case of the low inductive setup, while the over voltage peak height $V_{CE\,max} - V_{CE\,nom}$ is roughly 30% smaller for the XHP compared to the IVH-B.

In Figure 6 b), the normalized turn-off losses E_{off}/E_{max} of the XHP are plotted as a function of L_s for a constant, nominal dv/dt and nominal V_{CE} and I_C at T_j = 125°C. With the reduction of L_s from 300 nH (comparable to the IHV-B with L_s = 90 nH) to 85 nH E_{off} decreases by 5.5%. For T_j = 125°C the decrease of E_{off} over the same range of L_s amounts to 9%. Similar to the dynamic losses at turn-on a further decrease of E_{off} is possible by the choice of a faster IGBT.

In sum, the total dynamic losses for a typical XHP based converter under nominal conditions at T_j = 125°C are reduced by nearly 10% compared to a typical IHV-B based system. Potential for a further reduction of dynamic losses lies in the choice of faster IGBT and diode chips.

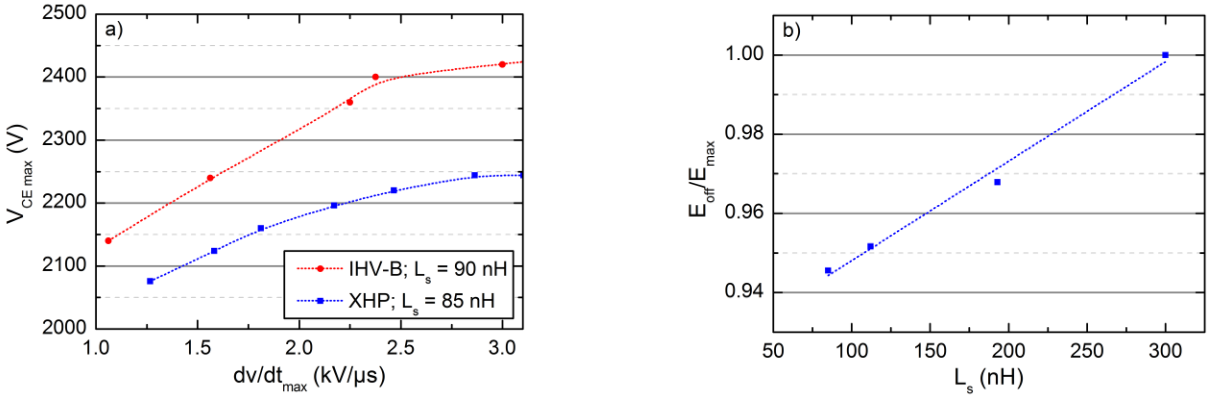

Figure 6: Comparison of the over voltage peak $V_{CE\,max}$ at IGBT turn-off as a function of the maximum dv/dt_{max} for the XHP and the IHV-B setup

a) nominal V_{CE} and I_C at T_j = 125°C

b) Normalized turn-off losses E_{off}/E_{max} as a function of the total commutation inductance L_s for the XHP, determined for the same nominal dv/dt at nominal V_{CE} and I_C at T_j = 125°C

Conclusion

The XHP module has been introduced as the new housing platform for high voltage IGBTs. With its modular half bridge design system scalability and reduced converter cost are addressed. State-of-the-art joining techniques and a low inductance concept prepare for the integration of the next chip technologies like wide bandgap semiconductors. The high voltage XHP HV package is designed to house chips of the voltage classes 3.3 to 6.5 kV with an insulation voltage of up to 10.4 kV.

Compared with today's module standard FZ1500R33HE3 in the single switch IHV-B package the presented 450 A rated 3.3 kV XHP HV features 17% higher power density and enables a reduction of the total stray inductance in a typical converter application by more than 70%. Beside an improved oscillation behavior the latter feature yields a reduction of nearly 10% total dynamic losses.